

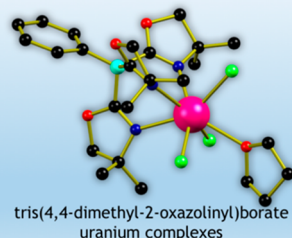
Low- and Mid-Valent Uranium Species Supported by Phenyltris(oxazolinyl)borate Ligands

Caleb J. Tatebe,^{1D} Ellen M. Matson,^{1D} Christopher L. Clark, John J. Kiernicki, Phillip E. Fanwick, Matthias Zeller,^{1D} and Suzanne C. Bart*^{1D}

H.C. Brown Laboratory, Department of Chemistry, Purdue University, West Lafayette, Indiana 47907, United States

Supporting Information

ABSTRACT: The synthesis and characterization of a family of uranium derivatives featuring the phenyltris(4,4-dimethyl-2-oxazolinyl)borate (To^M) ligand framework was achieved. Uranium(IV) halide compounds, specifically $To^M\text{UCl}_2(\text{THF})$ and $To^M\text{UI}_3$, were generated by adding 1 equiv of $\text{Ti}[To^M]$ to either UCl_4 or $\text{UI}_3(\text{THF})_4$, respectively. The tetravalent derivatives $To^M\text{UCl}_2(\text{NPh}_2)$ and $To^M\text{UI}(=\text{N-Ad})(\text{THF})$ were also synthesized, showing that To^M supports uranium amido and imido species. Attempts to make bis(phenyltris(oxazolinyl)borate) compounds were unsuccessful. However, when the smaller hydrotris(pyrazolyl)borate (Tp) ligand was used, a mixed bis(ligand) derivative, $TpTo^M\text{UI}$, was isolated. All of the compounds were characterized by ^1H NMR, infrared, and electronic absorption spectroscopies. Where possible, X-ray crystallography was used to assess structural parameters.



INTRODUCTION

Scorpionate ligands, first popularized by Trofimenko, have been used on virtually every metal on the periodic table.^{1–4} While these ligands are named for their tridentate coordination mode, scorpionates are considered to be analogous to cyclopentadienes, as both are monoanionic, six-electron donors (ionic model) and three-coordinate (one σ bond, two π bonds). In the years since the report of Trofimenko's poly(pyrazolyl)borate ligands,^{1–3,5} there have been many variations of this framework developed, including substituted poly(pyrazolyl)borate,^{6,7} poly(triazolyl)borate,^{8–10} poly(tetrazolyl)borate,^{11,12} poly(imazolyl)borate,¹³ and poly(alkyl phosphinyl)borate ligands,^{14,15} to tailor the steric and electronic properties of the resulting coordination complexes.

Sadow and co-workers have explored the utility of a variant of this class of ligands. Work from that laboratory has summarized the coordination chemistry of tris(oxazolinyl)borate ligands on various elements,^{16–22} including transition,^{17,22} main-group,¹⁸ and lanthanide¹⁹ metals. These ligands are readily tuned to suit both electronic and steric demands, as different oxazoline rings can be easily prepared from commercially available starting materials.²³ Enantiopure amino acids and/or alcohols allow for the preparation of chiral variants using inexpensive materials, as these building blocks are readily available.^{21,24} Furthermore, the incorporation of the B–C bonds in the oxazoline-based system is advantageous over the of B–N bonds typically found in pyrazole-based scorpionates, as the latter class is prone to borotropic shifting upon metalation.³

Coupled with our previous experiences with hydrotris(3,5-dimethylpyrazolyl)borate (Tp^*)^{25–40} and hydrotris(3-phenylpyrazolyl)borate (Tp^{Ph})⁴¹ ligands on uranium, we hypothesized that the chemistry of the phenyltris(4,4-dimethyl-2-oxazolinyl)borate (To^M) ligand framework would follow suit and may allow access to chiral variants of low-valent organoactinide complexes. Herein we report our entry into the synthesis and characterization of uranium(III) and uranium(IV) derivatives of the To^M ligand, including their reactivity. All species were characterized by ^1H NMR, infrared, and electronic absorption spectroscopies. For selected compounds, structural characterization by X-ray crystallography was obtained and is also discussed.

RESULTS AND DISCUSSION

Our studies commenced with the use of the To^M ligand, as the synthesis is straightforward from commercially available materials.⁴² As a previous investigation from our laboratory³³ has shown difficulty with the separation of trivalent uranium complexes from lithium salts, we chose to probe the synthesis of the $To^M\text{U}$ derivatives utilizing the thallium salt of the ligand, $\text{Ti}[To^M]$. This synthetic strategy has also been invoked by Sadow and co-workers for the coordination of the To^M ligand to a variety of metal centers.²² Treating a THF solution of UCl_4 with 1 equiv of $\text{Ti}[To^M]$ showed the formation of insoluble thallium chloride after 5 min, turning the solution to a suspension (Scheme 1, right). After 30 min of stirring and

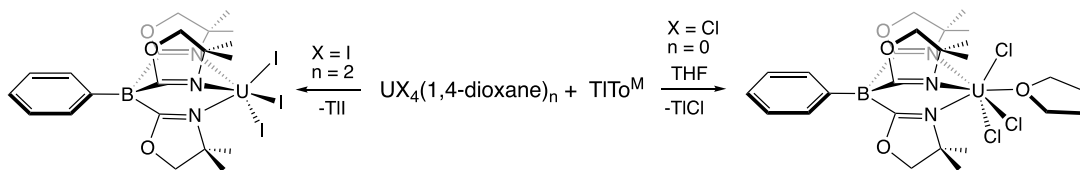
Received: November 21, 2019

Published: January 7, 2020



ACS Publications

© 2020 American Chemical Society

Scheme 1. Synthesis of $\text{To}^{\text{M}}\text{UCl}_3(\text{THF})$ and $\text{To}^{\text{M}}\text{UI}_3$ 

workup, the resulting green material was analyzed by ^1H NMR spectroscopy (benzene- d_6 , 23 °C), producing a spectrum that displayed seven paramagnetically broadened and shifted resonances ranging from -0.93 to 9.68 ppm, consistent with metalation of the ligand on U(IV). Two of these resonances were broad and in the region where free THF would be observed; thus, the product was assigned as $\text{To}^{\text{M}}\text{UCl}_3(\text{THF})$ (88% yield). Analysis of this pale green solid by IR spectroscopy (KBr pellet) revealed an absorption at 1548 cm^{-1} , consistent with the $\text{C}=\text{N}$ stretch of a metal-bound To^{M} ligand, as reported by Sadow and co-workers.¹⁹

To unambiguously confirm the coordination environment of the first isolated To^{M} actinide species, $\text{To}^{\text{M}}\text{UCl}_3(\text{THF})$, X-ray crystallography was utilized. Pale green crystals were grown from a concentrated solution of THF and toluene at $-35\text{ }^{\circ}\text{C}$. Refinement of structural data revealed a seven-coordinate uranium center with a $\kappa^3\text{-To}^{\text{M}}$ ligand, three chlorides, and a THF ligand in a distorted-monocapped-octahedral geometry (Figure 1 and Table 1). The U–N distances of

$\text{To}^{\text{M}}\text{UCl}_3(\text{THF})$ range from $2.448(6)$ to $2.511(5)\text{ \AA}$ and are similar to those of other reported U(IV) complexes ($\text{Tp}^*\text{UCl}_2[\text{NC}(\text{Ph})(\text{CH}_2\text{SiMe}_3)]$, $2.48(2)$ – $2.536(19)\text{ \AA}$;⁴³ $\text{Tp}^*\text{UCl}_2(\text{NEt}_2)$, $2.483(10)$ – $2.518(10)\text{ \AA}$; $\text{Tp}^{\text{Mes}}\text{UCl}_3$, $2.43(3)$ – $2.51(3)\text{ \AA}$;⁴⁴ $\text{Tp}^*\text{UCl}(\text{OPh})_2(\text{THF})$, $2.475(11)$ – $2.556(12)\text{ \AA}$;⁴⁵ $\text{Tp}^*\text{UCl}_3(\text{THF})$, $2.466(5)$ – $2.497(5)\text{ \AA}$).⁴⁶ The U–O_{THF} distance of $2.576(7)\text{ \AA}$ is similar to those of other U(IV)–THF compounds, including $\text{Tp}^*\text{UCl}_3(\text{THF})$ ($2.546(4)\text{ \AA}$).⁴⁶ The U–Cl distances of $2.5915(14)$, $2.6175(16)$, and $2.6240(15)\text{ \AA}$ are consistent with U(IV)–Cl distances in hydrotris(pyrazolyl)borate uranium trichloride species with varying pyrazole substituents, such as $\text{Tp}^*\text{UCl}_2(\text{NPh}_2)$ ($2.603(4)$, $2.608(4)\text{ \AA}$),⁴³ $\text{Tp}^*\text{UCl}_3(\text{THF})$ ($2.599(2)$, $2.609(2)$, $2.613(2)\text{ \AA}$),⁴⁶ and $\text{TpUCl}_3(\text{OP}(\text{OC}_2\text{H}_5)_3)$ ($2.610(4)$, $2.614(3)$, $2.618(4)\text{ \AA}$).⁴⁷

To assess the generality of this salt metathesis method for coordination of To^{M} to uranium(IV), the analogous iodide species was also synthesized. Addition of 1 equiv of $\text{TI}[\text{To}^{\text{M}}]$ to a solution of $\text{UI}_4(1,4\text{-dioxane})_2$ in toluene caused a gradual color change from orange to yellow with concurrent precipitation of thallium iodide (Scheme 1, left). After workup, the product was isolated as a yellow solid in moderate yield (62%), tentatively assigned as $\text{To}^{\text{M}}\text{UI}_3$.

Analysis of $\text{To}^{\text{M}}\text{UI}_3$ by ^1H NMR spectroscopy (benzene- d_6 , 25 °C) revealed five paramagnetically shifted resonances ranging from -2.41 to 11.66 ppm, with the largest, most upfield signal (18H) corresponding to the dimethyl moiety. The remaining resonances of the To^{M} ligand display a splitting pattern similar to that of $\text{To}^{\text{M}}\text{UCl}_3(\text{THF})$, with phenyl resonances located downfield at 8.67 , 9.07 , and 11.66 ppm and a resonance integrating to 6H for the $-\text{CH}_2$ group of the oxazoline rings at 3.32 ppm. ^{11}B NMR spectroscopy of $\text{To}^{\text{M}}\text{UI}_3$ showed a single broad resonance at 1.80 ppm, further indicative of a single product in solution. IR spectroscopy revealed a $\text{C}=\text{N}$ stretch at 1554 cm^{-1} , consistent with coordination of To^{M} to a metal.¹⁹ Unfortunately, suitable crystals for X-ray diffraction could not be obtained, precluding characterization of this species in the solid state. However, combustion analysis confirmed the elemental composition of $\text{To}^{\text{M}}\text{UI}_3$.

Next, we evaluated the suitability of these new metalated To^{M} derivatives as starting materials for further chemistry. A uranium amide species was first targeted, given the demonstrated utility of these ligands to support the uranium centers over years of study of actinide coordination chemistry.^{48–50} The most common synthetic route for metal amides is typically salt metathesis, which was demonstrated here by treating $\text{To}^{\text{M}}\text{UCl}_3(\text{THF})$ with 1 equiv of KNPh_2 in toluene, affording an orange powder (eq 1). Analysis of this

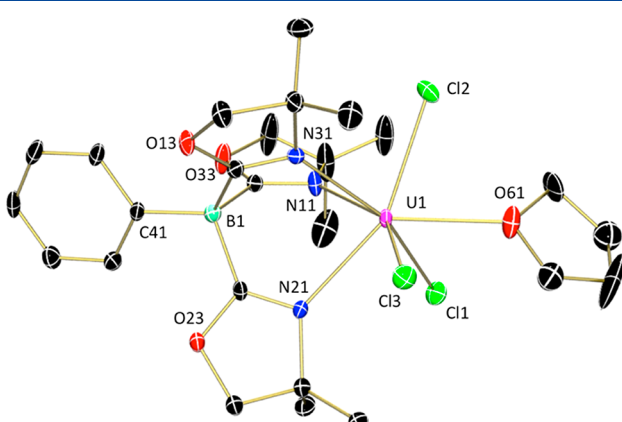
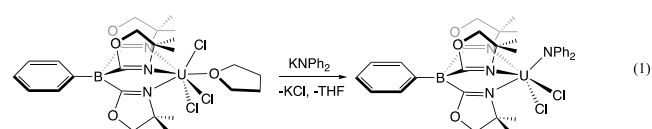


Figure 1. Molecular structure of $\text{To}^{\text{M}}\text{UCl}_3(\text{THF})$ shown with 30% probability ellipsoids. Hydrogen atoms and cocrystallized solvent molecules have been omitted for clarity.

Table 1. Bond Distances of To^{M} Uranium Derivatives (in \AA)

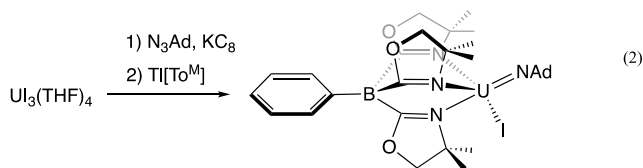
	$\text{To}^{\text{M}}\text{UCl}_3(\text{THF})$	$\text{To}^{\text{M}}\text{UI}(\text{--NAd})(\text{THF})$	$\text{TpTo}^{\text{M}}\text{UI}$
U1–Cl1	2.6240(15)		
U1–Cl2	2.6175(16)		
U1–Cl3	2.5915(14)		
U1–N1(1)	2.511(5)	2.526(15)	2.610(7)
U1–N2(1)	2.498(5)	2.54(4)	2.527(7)
U1–N3(1)	2.448(6)	2.645(16)	2.607(7)
U–N _{imido}		1.972(14)	
U–I(1)		3.1312(16)	3.222(6)
U1–N5			2.520(7)
U1–N7			2.557(7)
U1–N9			2.607(8)



powder by ^1H NMR spectroscopy (benzene- d_6 , 23 °C) showed paramagnetically shifted resonances ranging from –11 to 27 ppm. Three resonances (6H each) corresponded to the geminal methyl groups, whereas three resonances (2H) were assigned to the protons on the 5-position of the oxazoline rings, suggesting C_s symmetry of the product. $\text{To}^{\text{M}}\text{UCl}_2(\text{NPh}_2)$ is stable in benzene at room temperature, with ^1H NMR spectroscopy showing no noticeable decomposition over 1 week. The infrared spectrum of a KBr pellet of this material showed an absorption at 1545 cm $^{-1}$, corresponding to $\nu(\text{C}=\text{N})$.

Structural confirmation of $\text{To}^{\text{M}}\text{UCl}_2(\text{NPh}_2)$ was performed through crystallographic analysis of single, X-ray-quality crystals obtained by slow diffusion of pentane into a concentrated dichloromethane solution at –35 °C (Figure S5). While refinement of these data did reveal a uranium ion with two chloride, a diphenyl amide, and To^{M} ligand, the quality of the data was not sufficient to include a meaningful discussion of bond metrics.

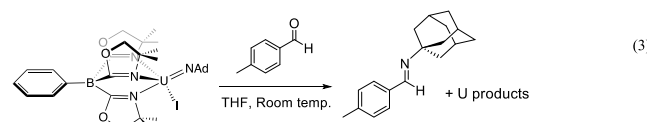
With successful synthesis of the amide derivative, a uranium(IV) imido species was also targeted to probe the stability of these ligands to support multiple-bond chemistry. Synthesis of such a derivative was achieved by treating a THF solution of $\text{UI}_3(\text{THF})_4$ with 1-azidoadamantane (N_3Ad) followed by KC_8 , yielding a brown solution (eq 2). To this



mixture was added a solution of $\text{Tl}[\text{To}^{\text{M}}]$ in THF dropwise, and following workup, a red-orange solid was isolated in high yield (93%). ^1H NMR spectroscopic analysis of this red-orange solid (benzene- d_6 , 23 °C) revealed a clean compound with a complicated spectrum with sharp resonances ranging from –40 to 65 ppm (details in the Experimental Section), as expected given the complexity of the adamantyl substituent. An absorption at 1560 cm $^{-1}$ was noted in the infrared spectrum of this material (KBr pellet).

Following solution characterization, crystals of the red-orange material suitable for single-crystal X-ray diffraction were obtained from a concentrated THF solution at –35 °C (Figure 2, left, and Table 1). Refinement of the data revealed a six-coordinate uranium center with one $\kappa^3\text{-To}^{\text{M}}$ ligand, one iodide, one THF molecule, and an adamantyl imido ligand, $\text{To}^{\text{M}}\text{UI}(\text{=N-Ad})(\text{THF})$. The $\text{U}-\text{N}_{\text{oxazolinyl}}$ distances (2.526(15)–2.645(16) Å) are similar to those observed for $\text{To}^{\text{M}}\text{UCl}_3(\text{THF})$ (Table 1) and $\text{Tp}^*\text{U}(\text{Bn})(\text{N-Mes})(\text{THF})$ (2.542(6)–2.634(6) Å),³² supporting the uranium(IV) oxidation state in this species. The $\text{U}-\text{N}_{\text{imido}}$ bond length of 1.972(14) Å is also similar to previously reported bis(Tp^*) uranium(IV) imido $\text{U}-\text{N}_{\text{imido}}$ distances ($\text{Tp}^*_{\text{2}}\text{U}(\text{N-Mes})$, 1.976(3) Å;²⁹ $\text{Tp}^*_{\text{2}}\text{U}(\text{N-Bn})$, 1.972(3) Å).⁴⁰ Thus, the To^{M} ligand framework is able to support metal species with multiply bonded substituents.

Further reactivity of the uranium(IV) imido species was probed, given that the uranium–nitrogen multiple bond has been demonstrated to undergo $[2\pi + 2\pi]$ cycloaddition of carbonyls readily in previously studied bis(Tp^*) systems (eq 3). Subjecting a THF solution of $\text{To}^{\text{M}}\text{UI}(\text{=N-Ad})$ to 1 equiv



of *p*-tolualdehyde caused a color change from red-orange to light yellow. Following workup and removal of intractable uranium products, the ^1H NMR spectrum of the resulting residue (benzene- d_6) is consistent with the formation of the organic imine product in good yield.²⁹

Interested in probing the possibility of generating a bis(scorpionate) species derived of the ToM scaffold, we sought to generate bis(To^{M}) uranium complexes. Unfortunately, multiple attempts at synthesis of these species by adding 2 equiv of $\text{Tl}[\text{To}^{\text{M}}]$ to $\text{UI}_3(\text{THF})_4$ or UCl_4 or 1 equiv of $\text{Tl}[\text{To}^{\text{M}}]$ to $\text{To}^{\text{M}}\text{UCl}_3(\text{THF})$ or $\text{To}^{\text{M}}\text{UI}_3$ were not successful.

We hypothesized this could be due to the large cone angle associated with these tris(oxazolinyl)borate ligands and undertook an analysis using the Solid-G program⁵¹ to determine the extent of steric crowding of the uranium center.

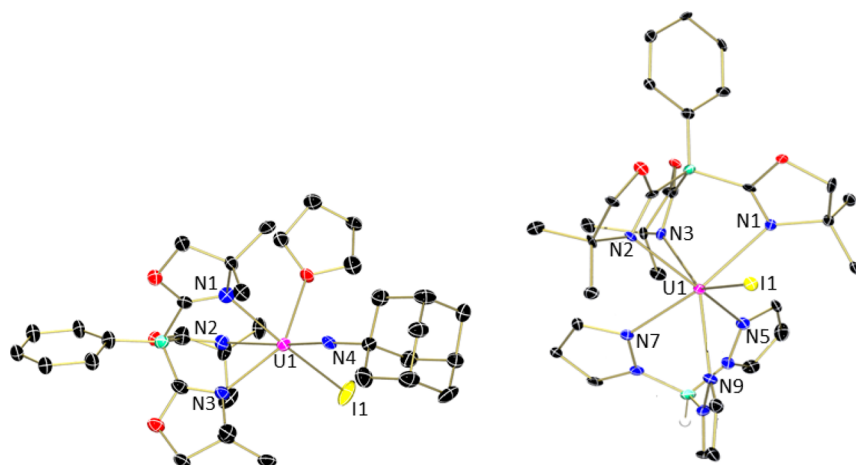


Figure 2. Molecular structure of $\text{To}^{\text{M}}\text{UI}(\text{=N-Ad})(\text{THF})$ (left) and $\text{Tp}^*\text{To}^{\text{M}}\text{UI}$ (right) shown with 30% probability ellipsoids. Hydrogen atoms and cocrystallized solvent molecules have been omitted for clarity.

Solid-G⁵¹ calculates the percentage of a metal's coordination sphere that is blocked by its ligand(s) on the basis of parameters obtained from experimental molecular structures, while also correcting for overlapping of adjacent ligands.

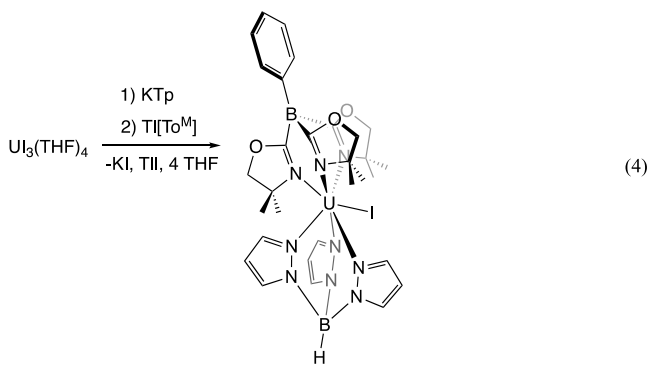
Solid-G analysis of $\text{To}^{\text{M}}\text{UCl}_3(\text{THF})$ shows that the To^{M} ligand itself consumes about 45% of the coordination sphere, whereas each halide consumes about 10% of the coordination sphere (Table 2). Therefore, two To^{M} ligands and a halide

Table 2. Solid-G⁵¹ Data for To^{M} Uranium Derivatives

	$\text{To}^{\text{M}}\text{UCl}_3(\text{THF})$	$\text{To}^{\text{M}}\text{UI}(=\text{N-Ad})(\text{THF})$	$\text{TpTo}^{\text{M}}\text{UI}$
$G(\text{To}^{\text{M}})$, %	45.07	45.13	43.60
$G(\text{X})$, %	$\text{X} = \text{Cl}$: 10.43, 10.38, 10.68	$\text{X} = \text{N-Ad}$: 18.18	$\text{X} = \text{Tp}$: 32.16
	$\text{X} = \text{THF}$: 12.43	$\text{X} = \text{I}$: 10.77	$\text{X} = \text{I}$: 10.08
		$\text{X} = \text{THF}$: 12.53	$\text{X} = \text{THF}$: 12.53
$G(\text{complex})$, %	86.13	85.23	84.80

would take up 100% of the coordination sphere. This is likely the reason that it has not been possible thus far to coordinate two To^{M} ligands to uranium.

Instead, a smaller scorpionate ligand, the parent hydrotris-(pyrazolyl)borate (Tp) ligand, was chosen to complete the coordination sphere. Given the smaller steric demands of this ligand, it should be possible to make a bis(ligand) species with To^{M} using this framework. The synthesis of the targeted mixed ligand species, $\text{TpTo}^{\text{M}}\text{UI}$, was achieved in high yield (86%) and purity by treating $\text{UI}_3(\text{THF})_4$ with 1 equiv of KTP (eq 4). After the mixture was stirred in THF for 30 min, a THF solution of $\text{TI}[\text{To}^{\text{M}}]$ was added dropwise; stirring and workup yielded a purple solid.



Analysis of a benzene- d_6 solution of this purple powder by ^1H NMR spectroscopy revealed a paramagnetically shifted spectrum with eight resonances. A singlet is observed at -9.82 ppm (18H) corresponding to the geminal methyl groups of the To^{M} ligand, whereas the methylene protons of the oxazolinyl backbone are displayed as a singlet (6H) at 3.44 ppm. Three resonances for the phenyl group on the boron of To^{M} appear at 8.97 ppm for the para proton of the phenyl ring (1H triplet), at 9.37 ppm (2H triplet) for the meta protons, and at 13.01 ppm (2H doublet) for the ortho protons. Three singlets (3H each) are observed ($-3.77, 8.16, 18.31$ ppm) and are assigned as the protons on the pyrazole ring. By ^{11}B NMR spectroscopy (benzene- d_6 , 25 °C; Figure S10), two broad resonances are observed ($-14, 40$ ppm) that correspond to two different boron-containing ligands bound to uranium. Analysis of $\text{TpTo}^{\text{M}}\text{UI}$ by IR spectroscopy (KBr pellet) displayed one

stretch for the B–H of Tp (2464 cm^{-1}) and one stretch for To^{M} 's C=N bond (1562 cm^{-1}).

Structural parameters of $\text{TpTo}^{\text{M}}\text{UI}$ were examined through an X-ray crystallographic analysis on suitable crystals obtained from slow diffusion of pentane into a concentrated THF solution at -35 °C (Figure 2, right; Table 1). The molecular structure obtained from refinement of the data displayed a seven-coordinate uranium center with an iodide atom, one κ^3 -Tp ligand, and one κ^3 - To^{M} ligand. For the To^{M} ligand, $\text{U}-\text{N}_{\text{oxazolinyl}}$ ($2.527(7)$ – $2.610(7)$ Å) bond lengths are in the same range as for $\text{To}^{\text{M}}\text{UI}(=\text{N-Ad})(\text{THF})$ (Table 1), whereas the $\text{U}-\text{N}_{\text{pyrazolyl}}$ bond lengths ($2.520(7)$ – $2.607(8)$ Å) of the Tp ligand are similar to the $\text{U}-\text{N}_{\text{pyrazolyl}}$ bond lengths reported for TpTp^*UBn (Bn = benzyl; $2.556(13)$ – $2.260(11)$ Å) and $\text{TpCp}^*\text{U}(\text{CH}_2\text{SiMe}_3)$ (Cp^* = pentamethylcyclopentadienide; $2.556(13)$ – $2.620(11)$ Å), which also feature U(III) mixed-ligand systems.³⁶

A Solid-G analysis of $\text{TpTo}^{\text{M}}\text{UI}$ further demonstrates the steric influence of the To^{M} ligand (Table 2). In this case, the To^{M} ligand still consumes over 40% of the coordination sphere, but the Tp ligand only uses about 32% in comparison. Coupled with the $\sim 10\%$ for the iodide ligand, the total steric demand for $\text{TpTo}^{\text{M}}\text{UI}$ is about 84%, which is in line with the other To^{M} derivatives. Thus, it is not sterically feasible to generate a bis(To^{M}) uranium species.

In order to assess the electronic structure of these species and confirm the oxidation states, all molecules were characterized using electronic absorption spectroscopy. Spectra were collected for each compound as a THF solution from 300 to 1800 nm at ambient temperature. In the near-infrared region, the spectra are consistent with those for typical uranium(IV) compounds,^{52,53} showing many sharp f–f transition absorbances that are weak in their molar absorptivity (~ 50 $\text{M}^{-1} \text{cm}^{-1}$) consistent with U(IV) $5f^2$ complexes (Figure 3, inset).^{52–54} The visible region shows more intense absorbances that are very broad, ranging from ~ 200 to 800 $\text{M}^{-1} \text{cm}^{-1}$ (Figure 3). $\text{To}^{\text{M}}\text{UI}_3$ shows an absorption at around 400 nm, which is likely responsible for its yellow appearance.

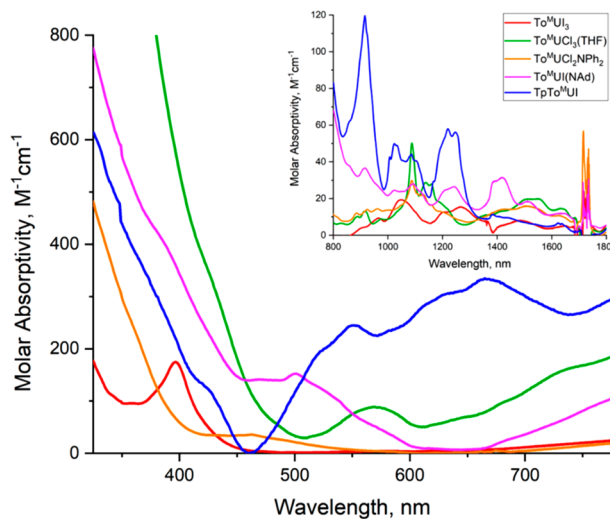


Figure 3. Electronic absorption spectra for $\text{To}^{\text{M}}\text{UI}_3$ (red), $\text{To}^{\text{M}}\text{UCl}_3(\text{THF})$ (green), $\text{To}^{\text{M}}\text{UCl}_3\text{NPh}_2$ (orange), $\text{To}^{\text{M}}\text{UI}(=\text{N-Ad})(\text{THF})$ (purple), and $\text{TpTo}^{\text{M}}\text{UI}$ (blue) in the visible region. Inset: electronic absorption data in the near-infrared and infrared regions. Solvent overtones are present between 1700 and 1800 nm.

Orange $\text{To}^{\text{M}}\text{UCl}_2\text{NPh}_2$ shows very weak absorbances around 450 nm as expected, whereas the absorbance for $\text{To}^{\text{M}}\text{UI}(=\text{N-Ad})(\text{THF})$ is shifted more toward ~ 500 nm, which is consistent with its red-orange appearance. In the case of $\text{TpTo}^{\text{M}}\text{UI}$, the uranium is trivalent rather than tetravalent, with an f^3 configuration; thus, the spectrum is strikingly different. In this case, there are broad absorptions throughout the visible region, including an intense one at ~ 650 nm which is likely responsible for the intense blue color. In the near-infrared region, $\text{TpTo}^{\text{M}}\text{UI}$ has characteristic absorptions for U(III) in which the absorbances are clearly higher in molar absorptivity in comparison to those for the U(IV) derivatives.

CONCLUSIONS

In summary, we have demonstrated that phenyltris(oxazolinyl) borate ligands are suitable for supporting uranium centers in both the +3 and +4 oxidation states. Using common uranium starting materials, metalation was achieved with the thallium derivative of the To^{M} ligand. Further reactivity was studied to assess the similarity of these ligands to traditional pyrazole-based scorpionate ligands. Both uranium(IV) amide and imido derivatives showed that these To^{M} ligands are sterically protective and robust to stay metalated during salt metathesis. This study has shown, however, that the large cone angle associated with the To^{M} ligand does not allow synthesis of the bis(ligand) derivative on a large metal such as uranium, in comparison to the bis(tris(pyrazolyl)borate) ligand architectures that are popular in the literature. Instead, the smaller unsubstituted hydrotris(pyrazolyl)borate, Tp , is required to generate a mixed bis(ligand) species. The brief steric analysis carried out here also demonstrates that this is a useful predictive tool for designing new ligand architectures. Future studies will build on this work with the synthesis and exploration of chiral variants of the tris(oxazolinyl)borate ligands.

EXPERIMENTAL SECTION

General Considerations. All air- and moisture-sensitive manipulations were performed using standard Schlenk techniques or using an MBraun inert-atmosphere drybox with an atmosphere of purified nitrogen. The MBraun drybox was equipped with a cold well designed for freezing samples in liquid nitrogen, as well as two -35 °C freezers for cooling samples and crystallizing compounds. Diethyl ether, pentane, tetrahydrofuran, and toluene for sensitive manipulations were dried and deoxygenated using literature procedures with a Seca solvent purification system.⁵⁵ Benzene- d_6 and chloroform- d were purchased from Cambridge Isotope Laboratories, dried with molecular sieves (C_6D_6 , CDCl_3) and sodium (C_6D_6), and degassed by three freeze-pump-thaw cycles. 1-Azidoadamantane was purchased from Sigma-Aldrich and used as received. Potassium graphite,⁵⁶ $\text{Ti}[\text{To}^{\text{M}}]$,²² KTP ,⁵⁷ UCl_4 ,⁵⁸ $\text{UI}_3(\text{THF})_4$,⁵⁹ and $\text{UI}_4(1,4\text{-dioxane})_2$,⁵⁹ were prepared using previously reported methods. KNPh_2 was prepared by treating diphenylamine with benzylpotassium.

^1H NMR spectra were recorded on a Varian Inova 300 spectrometer operating at 299.992 MHz. ^{11}B NMR spectra were recorded on a Varian Inova 300 spectrometer operating at a frequency of 96.24 MHz. All chemical shifts are reported relative to the peak for SiMe_4 , using ^1H residual chemical shifts of the solvent as a secondary standard. ^{11}B chemical shifts are reported relative to the peak for $\text{BF}_3\text{-Et}_2\text{O}$. The spectra for paramagnetic molecules were obtained using an acquisition time of 0.5 s; thus, the peak widths reported have an error of ± 2 Hz. For paramagnetic molecules, the ^1H NMR data are reported with the chemical shift, followed by the peak width at half-height in hertz, the integration value, and, where possible, the peak assignment. Elemental analyses were performed by Complete Analysis

Laboratories, Inc., Parsippany, NJ, or Midwest Microlab, Indianapolis, IN. Solid-state infrared spectra were recorded using a Thermo Nicolet iSS spectrophotometer; samples were made by crushing the solids, mixing with dry KBr , and pressing into a pellet. Electronic absorption spectroscopic measurements were recorded at 294 K in sealed 1 cm quartz cuvettes with a Cary 6000i UV-vis-NIR spectrophotometer.

Single-crystal data for $\text{To}^{\text{M}}\text{UCl}_3(\text{THF})$, $\text{To}^{\text{M}}\text{UI}(=\text{N-Ad})(\text{THF})$, and $\text{TpTo}^{\text{M}}\text{UI}$ were collected using a Rigaku R-axis curved image plate diffractometer as described in the *Supporting Information*. Full details, in CIF format, have been deposited with the Cambridge Crystallographic Data Centre (CCDC) with file numbers 1949524–1949526.

Synthesis of $\text{To}^{\text{M}}\text{UCl}_3(\text{THF})$. A 20 mL scintillation vial was charged with UCl_4 (0.500 g, 1.316 mmol) and approximately 7 mL of THF. A second vial was charged with $\text{Ti}[\text{To}^{\text{M}}]$ (0.772 g, 1.316 mmol) and approximately 3 mL of THF. The $\text{Ti}[\text{To}^{\text{M}}]$ solution was added dropwise to the stirred UCl_4 solution at room temperature. TiCl was produced within 5 min, and the reaction mixture was stirred for an additional 30 min. The resulting suspension was filtered, and the volatiles were removed in vacuo. The green solid was washed with pentane and dried under vacuum (0.768 g, 0.961 mmol, 73% yield). X-ray-quality crystals were grown from a concentrated solution of THF and toluene at -35 °C. Anal. Calcd for $\text{C}_{25}\text{H}_{37}\text{N}_3\text{O}_4\text{BUCl}_3$: C, 37.59; H, 4.67; N, 5.26. Found: C, 38.36; H, 5.05; N, 5.46. ^1H NMR (C_6D_6 , 25 °C): δ –0.93 (5, 18H, $(\text{CH}_3)_2$), 1.38 (48, 8H, THF), 3.31 (4, 6H, CH_2), 3.45 (53, 8H, THF), 7.96 (8, 1H, Ph-CH), 8.24 (t, J = 9, 2H, Ph-CH), 9.68 (d, J = 9, 2H, Ph-CH). IR: 1548 cm^{-1} (C=N).

Synthesis of $\text{To}^{\text{M}}\text{UI}_3$. A 20 mL scintillation vial was charged with $\text{UI}_4(\text{dioxane})_2$ (0.100 g, 0.108 mmol) and 7 mL of toluene. A second vial was charged with $\text{Ti}[\text{To}^{\text{M}}]$ (0.064 g, 0.108 mmol) in 3 mL of toluene. The $\text{Ti}[\text{To}^{\text{M}}]$ solution was added dropwise to the stirred UI_4 solution at ambient temperature. TII was observed immediately and after stirring for 30 min. The solution was filtered over Celite and washed with toluene to separate TII. Solvents were removed under reduced pressure, leaving the product, $\text{To}^{\text{M}}\text{UI}_3$, as a yellow powder (0.068 g, 0.068 mmol, 62%). Anal. Calcd for $\text{C}_{25}\text{H}_{37}\text{Bi}_3\text{N}_3\text{O}_4\text{U}$ (THF adduct): C, 27.98; H, 3.48; N, 3.92. Found: C, 28.46; H, 3.05; N, 4.12. ^1H NMR (benzene- d_6 , 25 °C): δ –2.41 (3, 18H, $(\text{CH}_3)_2$), 3.32 (2, 6H, CH_2), 8.67 (3, 1H, Ph-CH), 9.07 (2, 2H, Ph-CH), 11.66 (4, 2H, Ph-CH). No THF resonances are visible, likely due to the fluxionality of THF association/dissociation. ^{11}B NMR (CDCl_3 , 25 °C): δ 1.80. IR: 1554 cm^{-1} (C=N).

Synthesis of $\text{To}^{\text{M}}\text{UCl}_2(\text{NPh}_2)$. A 20 mL scintillation vial was charged with $\text{To}^{\text{M}}\text{UCl}_3(\text{THF})$ (0.125 g, 0.156 mmol) in 4 mL of toluene. To this light green solution was added KNPh_2 (0.032 g, 0.156 mmol), and the resulting suspension changed from yellow to orange. After the mixture was stirred for 2 h, KCl was removed by filtration and the orange solution was then concentrated under reduced pressure. Crystals were obtained by slow diffusion of pentane into a concentrated dichloromethane solution at -35 °C (Figure S5) but were not of sufficient quality to obtain a publishable data set. Anal. Calcd for $\text{C}_{33}\text{H}_{39}\text{BCl}_2\text{N}_4\text{O}_3\text{U}$: C, 46.12; H, 4.57; N, 6.52. Found: C, 45.97; H, 4.63; N, 6.38. ^1H NMR (C_6D_6 , 25 °C): δ –10.52 (3, 6H, $\text{To}^{\text{M}}\text{-}(2 \times \text{CH}_3)$), –3.96 (d, 2H, $\text{To}^{\text{M}}\text{-CH}_2$), –3.57 (d, 2H, $\text{To}^{\text{M}}\text{-CH}_2$), –0.17 (3, 6H, $\text{To}^{\text{M}}\text{-}(2 \times \text{CH}_3)$), 5.53 (t, 2H, *ortho*-CH), 5.80 (t, 1H, *para*-CH), 7.87 (9, 10H, N-Ph), 18.24 (3, 2H, $\text{To}^{\text{M}}\text{-CH}_2$), 26.91 (5, 6H, $\text{To}^{\text{M}}\text{-}(2 \times \text{CH}_3)$). IR (KBr): $\nu_{\text{C}=\text{N}}$ 1545 cm^{-1} .

Synthesis of $\text{To}^{\text{M}}\text{UI}(=\text{N-Ad})(\text{THF})$. A 20 mL scintillation vial was charged with $\text{UI}_3(\text{THF})_4$ (0.100 g, 0.110 mmol) and 2 mL of THF. A second vial was charged with 1-azidoadamantane (0.020 g, 0.110 mmol) and 2 mL of THF, and this colorless solution was added to the first vial, giving a purple solution. While this mixture was stirred, KC_8 (0.015 g, 0.110 mmol) was slowly added to the purple solution; an additional 15 min of stirring yielded a brown solution. At this juncture, a solution of $\text{Ti}[\text{To}^{\text{M}}]$ (0.065 g, 0.110 mmol) in 3 mL of THF was added dropwise to the brown solution. After the mixture was stirred for 2 h, KI , TII, and graphite were filtered out and volatiles were removed in vacuo. The resulting red-orange solid was washed with pentane (2 \times 5 mL) and dried under vacuum (0.098 g, 0.102 mmol, 93% yield). Single X-ray-quality crystals were obtained from a

concentrated solution of THF at -35°C . ^1H NMR (C_6D_6 , 25°C): δ -40.07 (8 , 6H , $\text{To}^{\text{M}}\text{-}(2 \times \text{CH}_2)$), -25.21 (2H , $\text{To}^{\text{M}}\text{-}(2 \times \text{H})$), -24.03 (2H , $\text{To}^{\text{M}}\text{-}(2 \times \text{H})$), -9.5 (6H , $\text{To}^{\text{M}}\text{-}(2 \times \text{CH}_3)$), 7.5 (1H , *para*-CH), 7.62 (2H , *meta*-CH), 7.80 (2H , *ortho*-CH), 20.79 (3H , Ad-CH), 26.32 (3H , Ad-CH), 28.48 (13 , 3H , Ad-CH), 56.3 (9 , 6H , Ad-CH), 59.24 (2H , $\text{To}^{\text{M}}\text{-}(2 \times \text{H})$), 65.41 (9 , 6H , $\text{To}^{\text{M}}\text{-}(2 \times \text{CH}_3)$). ^{11}B NMR (C_6D_6 , 25°C): δ 26.07 . IR (KBr): $\nu_{\text{C}=\text{N}}$ 1560 cm^{-1} .

Synthesis of $\text{TpTo}^{\text{M}}\text{UI}$. A 20 mL scintillation vial was charged with $\text{UI}_3(\text{THF})_4$ (0.500 g , 0.551 mmol) and 10 mL of THF. KTP (0.139 g , 0.551 mmol) was added to the rapidly stirred solution. The resulting mixture was stirred for 2 h to give a purple solution. At this time, $\text{Ti}[\text{To}^{\text{M}}]$ (0.324 g , 0.551 mmol) was dissolved in THF and added dropwise to the stirred solution of TpUI_2 . This solution was stirred for 2 h before filtration and removal of the volatiles in *vacuo* to give a blue solid. Washing with pentane and drying under vacuum gave a blue solid in 86% yield (0.455 g , 0.474 mmol). X-ray-quality crystals were obtained for this complex through slow diffusion of pentane into a concentrated THF solution at -35°C . Anal. Calcd for $\text{C}_{30}\text{H}_{39}\text{B}_2\text{IN}_9\text{O}_3\text{U}$: C, 37.52 ; H, 4.09 ; N, 13.13 . Found: C, 37.07 ; H, 4.20 ; N, 12.82 . ^1H NMR (C_6D_6 , 25°C): δ -9.62 (19 , 18H , $\text{To}^{\text{M}}\text{-}(6 \times \text{CH}_3)$), -3.77 (29 , 3H , Tp-CH), 3.44 (6H , $\text{To}^{\text{M}}\text{-}(3 \times 2\text{H})$), 8.16 (6 , 3H , Tp-CH), 8.97 (1H , *para*-CH), 9.37 (2H , *meta*-CH), 13.01 (2H , *ortho*-CH), 18.31 (25 , 3H , Tp-CH). No resonance for the H-B moiety could be located in the ^1H NMR spectrum due to the paramagnetic nature of this species. ^{11}B NMR (C_6D_6 , 25°C): δ 14 , 40 . IR (KBr): $\nu_{\text{B}-\text{H}}$ 2464 cm^{-1} ; $\nu_{\text{C}=\text{N}}$ 1562 cm^{-1} .

■ ASSOCIATED CONTENT

Supporting Information

The Supporting Information is available free of charge at <https://pubs.acs.org/doi/10.1021/acs.organomet.9b00793>.

Additional NMR and IR data, connectivity image of $\text{To}^{\text{M}}\text{UCl}_2(\text{NPh}_2)$, and tabulated X-ray parameters (PDF)

Accession Codes

CCDC 1949524–1949526 contain the supplementary crystallographic data for this paper. These data can be obtained free of charge via www.ccdc.cam.ac.uk/data_request/cif, or by emailing data_request@ccdc.cam.ac.uk, or by contacting The Cambridge Crystallographic Data Centre, 12 Union Road, Cambridge CB2 1EZ, UK; fax: +44 1223 336033.

■ AUTHOR INFORMATION

Corresponding Author

*E-mail for S.C.B.: sbart@purdue.edu.

ORCID

Caleb J. Tatebe: [0000-0002-7817-388X](http://orcid.org/0000-0002-7817-388X)

Ellen M. Matson: [0000-0003-3753-8288](http://orcid.org/0000-0003-3753-8288)

Matthias Zeller: [0000-0002-3305-852X](http://orcid.org/0000-0002-3305-852X)

Suzanne C. Bart: [0000-0002-8918-9051](http://orcid.org/0000-0002-8918-9051)

Notes

The authors declare no competing financial interest.

■ ACKNOWLEDGMENTS

This work was supported by the National Science Foundation (NSF) (CHE-1665170, S.C.B.). This material is also based upon work supported by the NSF through the Major Research Instrumentation Program under Grant CHE 1625543. The authors also acknowledge Derek Jorgensen for his contributions to THE preparation of LiTo^{M} .

■ REFERENCES

- Pettinari, C. Scorpionate Compounds. *Eur. J. Inorg. Chem.* **2016**, *2016*, 2209–2211.
- Trofimenko, S. *Scorpionates*; Imperial College Press: London, England, 1999.
- Trofimenko, S. Recent advances in poly(pyrazolyl)borate (scorpionate) chemistry. *Chem. Rev.* **1993**, *93*, 943–980.
- Trofimenko, S. Scorpionates: genesis, milestones, prognosis. *Polyhedron* **2004**, *23*, 197–203.
- Pettinari, C. *Scorpionates II: Chelating Borate Ligands*; Imperial College Press: London, England, 2008.
- van Dijkman, T. F.; Siegler, M. A.; Bouwman, E. Copper(I) Complexes of Naphthyl-Substituted Fluorinated Trispyrazolylborate Ligands with Ethene and Carbon Monoxide. *Eur. J. Inorg. Chem.* **2016**, *2016*, 2586–2594.
- Zhang, S.; Melzer, M. M.; Sen, S. N.; Çelebi-Ölçüm, N.; Warren, T. H. A motif for reversible nitric oxide interactions in metalloenzymes. *Nat. Chem.* **2016**, *8*, 663.
- Jernigan, F. E.; Sieracki, N. A.; Taylor, M. T.; Jenkins, A. S.; Engel, S. E.; Rowe, B. W.; Jové, F. A.; Yap, G. P. A.; Papish, E. T.; Ferrence, G. M. Sterically Bulky Tris(triazolyl)borate Ligands as Water-Soluble Analogues of Tris(pyrazolyl)borate. *Inorg. Chem.* **2007**, *46*, 360–362.
- Kumar, M.; Papish, E. T.; Zeller, M.; Hunter, A. D. Zinc complexes of TtzR , Me with O and S donors reveal differences between Tp and Ttz ligands: acid stability and binding to H or an additional metal (TtzR , Me = tris(3-R-5-methyl-1,2,4-triazolyl)borate; R = Ph, *t*Bu). *Dalton Trans* **2011**, *40*, 7517–7533.
- Pellei, M.; Santini, C.; Marinelli, M.; Trasatti, A.; Dias, H. V. R. The hydridotris(3-nitro-1,2,4-triazol-1-yl)borate, a new nitro-substituted electron withdrawing polydentate “scorpionate”-type ligand and related copper and silver phosphane complexes. *Polyhedron* **2017**, *125*, 86–92.
- Janiak, C.; Scharmann, T. G. Supramolecular C-H···O, C-H···N and C-H···Cl interactions in metal compounds with multi-topic poly(pyrazolyl)borate ligands. *Polyhedron* **2003**, *22*, 1123–1133.
- Lu, D.; Winter, C. H. Complexes of the $[\text{K}(18\text{-Crown-6})]^+$ Fragment with Bis(tetrazolyl)borate Ligands: Unexpected Boron-Nitrogen Bond Isomerism and Associated Enforcement of $\kappa^3\text{-N, N'}$ -H-Ligand Chelation. *Inorg. Chem.* **2010**, *49*, 5795–5797.
- Spicer, M. D.; Reglinski, J. Soft Scorpionate Ligands Based on Imidazole-2-thione Donors. *Eur. J. Inorg. Chem.* **2009**, *2009*, 1553–1574.
- Jenkins, D. M.; Betley, T. A.; Peters, J. C. Oxidative Group Transfer to Co(I) Affords a Terminal Co(III) Imido Complex. *J. Am. Chem. Soc.* **2002**, *124*, 11238–11239.
- Lu, C. C.; Peters, J. C. Catalytic Copolymerization of CO and Ethylene with a Charge Neutral Palladium(II) Zwitterion. *J. Am. Chem. Soc.* **2002**, *124*, 5272–5273.
- Baird, B.; Pawlikowski, A. V.; Su, J.; Wiench, J. W.; Pruski, M.; Sadow, A. D. Easily Prepared Chiral Scorpionates: Tris(2-oxazolinyl)-boratoiridium(I) Compounds and Their Interactions with MeOTf. *Inorg. Chem.* **2008**, *47*, 10208–10210.
- Dunne, J. F.; Su, J.; Ellern, A.; Sadow, A. D. A New Scorpionate Ligand: Tris(4,4-dimethyl-2-oxazolinyl)borate and Its Zirconium(IV) Complexes. *Organometallics* **2008**, *27*, 2399–2401.
- Neal, S. R.; Ellern, A.; Sadow, A. D. Optically active, bulky tris(oxazolinyl)borato magnesium and calcium compounds for asymmetric hydroamination/cyclization. *J. Organomet. Chem.* **2011**, *696*, 228–234.
- Pawlikowski, A. V.; Ellern, A.; Sadow, A. D. Ligand Exchange Reactions and Hydroamination with Tris(oxazolinyl)borato Yttrium Compounds. *Inorg. Chem.* **2009**, *48*, 8020–8029.
- Reinig, R. R.; Mukherjee, D.; Weinstein, Z. B.; Xie, W.; Albright, T.; Baird, B.; Gray, T. S.; Ellern, A.; Miller, G. J.; Winter, A. H.; Bud'ko, S. L.; Sadow, A. D. Synthesis and Oxidation Catalysis of [Tris(oxazolinyl)borato]cobalt(II) Scorpionates. *Eur. J. Inorg. Chem.* **2016**, *2016*, 2486–2494.

(21) Xu, S.; Magoon, Y.; Reinig, R. R.; Schmidt, B. M.; Ellern, A.; Sadow, A. D. Organometallic Complexes of Bulky, Optically Active, C3-Symmetric Tris(4S-isopropyl-5,5-dimethyl-2-oxazolinyl)-phenylborate ($\text{To}^{\text{P}*}$). *Organometallics* **2015**, *34*, 3508–3519.

(22) Ho, H.-A.; Dunne, J. F.; Ellern, A.; Sadow, A. D. Reactions of Tris(oxazolinyl)phenylborato Rhodium(I) with C-X (X = Cl, Br, OTf) Bonds: Stereoselective Intermolecular Oxidative Addition. *Organometallics* **2010**, *29*, 4105–4114.

(23) Mukherjee, D.; Ellern, A.; Sadow, A. D. Remarkably Robust Monomeric Alkylperoxyzinc Compounds from Tris(oxazolinyl)-boratozinc Alkyls and O_2 . *J. Am. Chem. Soc.* **2012**, *134*, 13018–13026.

(24) Evans, D. A.; Peterson, G. S.; Johnson, J. S.; Barnes, D. M.; Campos, K. R.; Woerpel, K. A. An Improved Procedure for the Preparation of 2,2-Bis[2-[4(S)-tert-butyl-1,3-oxazolinyl]]propane [(S, S)-tert-Butylbis(oxazoline)] and Derived Copper(II) Complexes. *J. Org. Chem.* **1998**, *63*, 4541–4544.

(25) Kiernicki, J. J.; Higgins, R. F.; Kraft, S. J.; Zeller, M.; Shores, M. P.; Bart, S. C. Elucidating the Mechanism of Uranium Mediated Diazene N = N Bond Cleavage. *Inorg. Chem.* **2016**, *55*, 11854–11866.

(26) Kraft, S. J.; Fanwick, P. E.; Bart, S. C. Synthesis and characterization of a uranium(III) complex containing a redox-active 2,2'-bipyridine ligand. *Inorg. Chem.* **2010**, *49*, 1103–1110.

(27) Kraft, S. J.; Walensky, J.; Fanwick, P. E.; Hall, M. B.; Bart, S. C. Crystallographic evidence of a base-free uranium(IV) terminal oxo species. *Inorg. Chem.* **2010**, *49*, 7620–7622.

(28) Matson, E. M.; Breshears, A. T.; Kiernicki, J. J.; Newell, B. S.; Fanwick, P. E.; Shores, M. P.; Walensky, J. R.; Bart, S. C. Trivalent uranium phenylchalcogenide complexes: exploring the bonding and reactivity with CS_2 in the $\text{Tp}^*{}_{\text{2}}\text{UEPh}$ series (E = O, S, Se, Te). *Inorg. Chem.* **2014**, *53*, 12977–85.

(29) Matson, E. M.; Crestani, M. P.; Fanwick, P. E.; Bart, S. C. Synthesis of U(IV) imidos from $\text{Tp}^*{}_{\text{2}}\text{U}(\text{CH}_2\text{Ph})$ (Tp^* = hydrotris(3,5-dimethylpyrazolyl)borate) by extrusion of bibenzyl. *Dalton Trans* **2012**, *41*, 7952–7958.

(30) Matson, E. M.; Fanwick, P. E.; Bart, S. C. Diazoalkane Reduction for the Synthesis of Uranium Hydrazonido Complexes. *Eur. J. Inorg. Chem.* **2012**, *2012*, 5471–5478.

(31) Matson, E. M.; Fanwick, P. E.; Bart, S. C. Formation of Trivalent U–C, U–N, and U–S Bonds and Their Reactivity toward Carbon Dioxide and Acetone. *Organometallics* **2011**, *30*, 5753–5762.

(32) Matson, E. M.; Forrest, W. P.; Fanwick, P. E.; Bart, S. C. Synthesis and Reactivity of Trivalent $\text{Tp}^*{}_{\text{2}}\text{U}(\text{CH}_2\text{Ph})_2(\text{THF})$: Insertion vs Oxidation at Low-Valent Uranium–Carbon Bonds. *Organometallics* **2013**, *32*, 1484–1492.

(33) Matson, E. M.; Forrest, W. P.; Fanwick, P. E.; Bart, S. C. Use of Alkylsodium Reagents for the Synthesis of Trivalent Uranium Alkyl Complexes. *Organometallics* **2012**, *31*, 4467–4473.

(34) Matson, E. M.; Goshert, M. D.; Kiernicki, J. J.; Newell, B. S.; Fanwick, P. E.; Shores, M. P.; Walensky, J. R.; Bart, S. C. Synthesis of terminal uranium(IV) disulfido and diselenido compounds by activation of elemental sulfur and selenium. *Chem. - Eur. J.* **2013**, *19*, 16176–16180.

(35) Matson, E. M.; Kiernicki, J. J.; Anderson, N. H.; Fanwick, P. E.; Bart, S. C. Isolation of a uranium(III) benzophenone ketyl radical that displays redox-active ligand behaviour. *Dalton Trans* **2014**, *43*, 17885–17888.

(36) Matson, E. M.; Kiernicki, J. J.; Fanwick, P. E.; Bart, S. C. Expanding the Family of Uranium(III) Alkyls: Synthesis and Characterization of Mixed-Ligand Derivatives. *Eur. J. Inorg. Chem.* **2016**, *2016*, 2527–2533.

(37) Tatebe, C. J.; Collins, T. S.; Barnett, G. R.; Zeller, M.; Bart, S. C. Preparation of U(IV) κ^1 -amidinate complexes by nitrile metathesis. *Polyhedron* **2019**, *158*, 1–7.

(38) Tatebe, C. J.; Johnson, S. A.; Zeller, M.; Bart, S. C. Generation of $\text{Tp}^*{}_{\text{2}}\text{U}(\text{N}_3)$ from a family of new uranium(III) alkyl complexes. *J. Organomet. Chem.* **2018**, *857*, 152–158.

(39) Tatebe, C. J.; Tong, Z.; Kiernicki, J. J.; Coughlin, E. J.; Zeller, M.; Bart, S. C. Activation of Triphenylphosphine Oxide Mediated by Trivalent Organouranium Species. *Organometallics* **2018**, *37*, 934–940.

(40) Tatebe, C. J.; Zeller, M.; Bart, S. C. [24 + 22] Cycloaddition of Isocyanates to Uranium(IV) Imido Complexes for the Synthesis of U(IV) N^2 -Ureato Compounds. *Inorg. Chem.* **2017**, *56*, 1956–1965.

(41) Johnson, S. A.; Tatebe, C. J.; Gonzalez, S.; Zeller, M.; Bart, S. C. Synthesis and characterization of hydrotris(3-phenylpyrazolyl)borate ligands on low-valent uranium. *Polyhedron* **2017**, *125*, 107–112.

(42) Mukherjee, D.; Thompson, R. R.; Ellern, A.; Sadow, A. D. Coordinatively Saturated Tris(oxazolinyl)borato Zinc Hydride-Catalyzed Cross Dehydrocoupling of Silanes and Alcohols. *ACS Catal.* **2011**, *1*, 698–702.

(43) Silva, M.; Antunes, M. A.; Dias, M.; Domingos, A.; dos Santos, I. C.; Marcalo, J.; Marques, N. The uranium–nitrogen bond in U(IV) complexes supported by the hydrotris(3,5-dimethylpyrazolyl)borate ligand. *Dalton Trans* **2005**, 3353.

(44) Silva, M.; Domingos, A.; Pires de Matos, A.; Marques, N.; Trofimienko, S. Hydrotris(mesitylpyrazol-1-yl)borate uranium(IV) compounds: synthesis, structure, and ligand isomerization. *Dalton Trans* **2000**, 4628–4634.

(45) Domingos, A.; Marcalo, J.; Marques, N.; Pires de Matos, A.; Takats, J.; Bagnall, K. W. Actinide poly(pyrazol-1-yl)borate complexes: Synthesis and characterization of hydrotris(3,5-dimethylpyrazol-1-yl)boratotrichlorotetrahydrofuran actinide(IV), $\text{M}[\text{HB}(3,5\text{-Me}_2\text{Pz})_3]\text{Cl}_3(\text{THF})$ ($\text{M} = \text{Th}$ and U). *Inorg. Chim. Acta* **1987**, *132*, 137–143.

(46) Maier, R.; Müller, J.; Kanellakopoulos, B.; Apostolidis, C.; Domingos, A.; Marques, N.; De Matos, A. P. Molecular structure and charge distribution in compounds of the 5f-elements—VI. 1:1 adducts of uranium(IV)-hydrotris(3,5-dimethylpyrazol-1-yl)borate-trichloride with Lewis bases. *Polyhedron* **1993**, *12*, 2801–2808.

(47) Stewart, J. L.; Andersen, R. A. Crystal structures of $[(\text{Me}_3\text{Si})_2\text{N}]_4\text{U}_2\text{[}-\text{N}(\text{H})(\text{mesityl})\text{]}_2$ and $[(\text{Me}_3\text{Si})_2\text{N}]_4\text{U}_2\text{[}-\text{N}(\text{p-tolyl})\text{]}_2$; compounds with asymmetrically bridging primary amide and imide groups. *New J. Chem.* **1995**, *19*, 587–595.

(48) Stewart, J. L.; Andersen, R. A. Trivalent uranium chemistry: molecular structure of $[(\text{Me}_3\text{Si})_2\text{N}]_3\text{U}$. *Polyhedron* **1998**, *17*, 953–958.

(49) Lewis, A. J.; Williams, U. J.; Carroll, P. J.; Schelter, E. J. Tetrakis(bis(trimethylsilyl)amido)uranium(IV): Synthesis and Reactivity. *Inorg. Chem.* **2013**, *52*, 7326–7328.

(50) Guzei, I. A.; Wendt, M. An improved method for the computation of ligand steric effects based on solid angles. *Dalton Trans* **2006**, 3991–9.

(51) Lam, O. P.; Anthon, C.; Heinemann, F. W.; O'Connor, J. M.; Meyer, K. Structural and Spectroscopic Characterization of a Charge-Separated Uranium Benzophenone Ketyl Radical Complex. *J. Am. Chem. Soc.* **2008**, *130*, 6567–6576.

(52) Kraft, S. J.; Williams, U. J.; Daly, S. R.; Schelter, E. J.; Kozimor, S. A.; Boland, K. S.; Kikkawa, J. M.; Forrest, W. P.; Christensen, C. N.; Schwarz, D. E.; Fanwick, P. E.; Clark, D. L.; Conradson, S. D.; Bart, S. C. Synthesis, characterization, and multielectron reduction chemistry of uranium supported by redox-active alpha-diimine ligands. *Inorg. Chem.* **2011**, *50*, 9838–9848.

(53) Bordreaux, E. A. M.; Mulay, L. N. *Theory and Applications of Molecular Paramagnetism*; Wiley: New York, 1976.

(54) Pangborn, A. B.; Giardello, M. A.; Grubbs, R. H.; Rosen, R. K.; Timmers, F. J. Safe and Convenient Procedure for Solvent Purification. *Organometallics* **1996**, *15*, 1518–1520.

(55) Chakraborty, S.; Chattopadhyay, J.; Guo, W.; Billups, W. E. Functionalization of Potassium Graphite. *Angew. Chem., Int. Ed.* **2007**, *46*, 4486–4488.

(57) Trofimenko, S.; Long, J. R.; Nappier, T.; Shore, S. G., Poly(1-pyrazolyl)borates, Their Transition-Metal Complexes, and Pyrazaboles. In *Inorganic Syntheses*; Parry, R. W., Ed.; Wiley: 1970; Vol. 12.

(58) Kiplinger, J. L.; Morris, D. E.; Scott, B. L.; Burns, C. J. Convenient Synthesis, Structure, and Reactivity of $(C_3Me_5)U(CH_2C_6H_5)_3$: A Simple Strategy for the Preparation of Monopentamethylcyclopentadienyl Uranium(IV) Complexes. *Organometallics* **2002**, *21*, 5978–5982.

(59) Monreal, M. J.; Thomson, R. K.; Cantat, T.; Travia, N. E.; Scott, B. L.; Kiplinger, J. L. $UI_4(1,4\text{-dioxane})_2$, $[UCl_4(1,4\text{-dioxane})]_2$, and $UI_3(1,4\text{-dioxane})_{1.5}$: Stable and Versatile Starting Materials for Low- and High-Valent Uranium Chemistry. *Organometallics* **2011**, *30*, 2031–2038.